

Development of FCC Matrix High Entropy Matrix Porous Alloy



By

**Habib Malik
Osama Bin Zia
Osama Farrukh**

**School of Chemical and Materials Engineering
National University of Sciences and Technology**

2020

Development of FCC Matrix High Entropy Matrix Porous Alloy



(Leader - 196251 Osama Bin Zia)

(Member 1 - 196251 Osama Bin Zia)

(Member 2 - 173707 Osama Farrukh)

(Member 3 - 176576 Habib Malik)

School of Chemical and Materials Engineering (SCME)
National University of Sciences and Technology (NUST)

July, 2020

CERTIFICATE

This is to certify that work in this thesis has been completed by Mr. Osama Bin Zia, Mr. Osama Farrukh and Mr. Habib Malik under the supervision of Dr. Khurram Yaqoob and Dr. Muhammad Aftab Akram at the school of Chemical and Materials Engineering (SCME), National University of Science and Technology, H-12, Islamabad, Pakistan.

Advisor:

Dr. Khurram Yaqoob
Department of Materials Engineering
School of Chemical and Materials
Engineering
National University of Sciences and
Technology

Co-Advisor (if any)

Dr. Muhammad Aftab Akram
Department of Materials Engineering
School of Chemical and Materials
Engineering
National University of Sciences and
Technology

Submitted Through:

HOD-----

Department of Materials Engineering
School of Chemical and Materials
Engineering
National University of Sciences and
Technology

Principal/Dean -----
School of Chemical and Materials
Engineering
National University of Sciences and
Technology

DEDICATION

We would like to thank our parents for providing us with the support and guidance that we needed throughout this project.

ABSTRACT

High-Entropy Alloys (HEA) consist of at least five or more principal elements having equimolar or near equimolar ratios. This emerging concept has established a fact that there is so much more yet to be discovered. Four core effects observed in HEAs which are entropic stabilization, sluggish diffusion, severe lattice distortion and cocktail effect enable them to exhibit extraordinary properties. Our aim was to utilize this idea and could address the problems faced with conventional alloys. We designed an FCC Matrix High-Entropy Porous Alloy and aimed to investigate its high-end properties and potential applications.

TABLE OF CONTENTS

DEDICATION.....	i
ABSTRACT.....	ii
LIST OF FIGURES.....	v
LIST OF TABLES.....	vi
CHAPTER 1	1
INTRODUCTION.....	1
1.1 High Entropy Alloys.....	1
1.2 Four Core Effects in HEAs	2
1.3 Entropic Stabilization	2
1.4 Sluggish Diffusion.....	3
1.5 Severe Lattice Distortion	5
1.6 Cocktail	6
1.7 Properties of HEAs	8
1.7.1 Mechanical Properties	8
1.7.2 Wear and Fatigue Properties	9
1.7.3 Elevated Temperature Properties.....	10
1.7. 4 Corrosion Properties	10
1.8 Potential Applications.....	10
1.8.1 Thermal Barrier Coatings	11
1.8.2 HardFacing Applications	11
1.8.3 Antibacterial and Electromagnetic Interference Shielding Coatings	12
CHAPTER 2	14
LITERATURE REVIEW	14
Chapter 3	20
EXPERIMENTAL PROCEDURES	20
3.1 Alloy Design	20
3.2 Cutting and Weighing of the Materials.....	21
3.3 Washing and cleaning.....	22
3.4 Arc Melting	22
3.5 Machining	24
3.6 XRD.....	25
3.7 SEM	26

3.7.1 Sample Preparation	26
3.7.2 Metallographic Mounting	26
3.7.3 Grinding.....	26
3.7.4 Polishing.....	26
3.7.5 Etching.....	27
CHAPTER 4	28
RESULTS AND DISCUSSION	28
4.1 Optical microscopy	28
4.2 Scanning Electron Microscopy.....	28
4.3 XRD.....	31
4.4 Weight loss measurement.....	32
CONCLUSION.....	33
References	34

LIST OF FIGURES

Figure 1.....	4
Figure 2.....	5
Figure 3.....	6
Figure 4.....	7
Figure 5.....	8
Figure 6.....	8
Figure 7.....	9
Figure 8.....	10
Figure 9.....	11
Figure 10.....	11
Figure 11.....	12
Figure 12.....	12
Figure 13.....	13
Figure 14 List of all possible elements that can be used in HEAs [5].....	14
Figure 15: Structure of AlCoCrFeNiSiTi alloy plasma sprayed on 304 Stainless Steel [2].	16
Figure 16: Schematic of LENS Technique [1].....	17
Figure 17: Analytical weighing balance.....	21
Figure 18: Sonication Bath	22
Figure 19: Layer by layer stacking of parent metals (left) closing the door of melting chamber and vacuum generation (right).....	23
Figure 20: Protective shield is up and arc is generated.....	24
Figure 21: 2D engineering drawing of the sample to be machined.....	25
Figure 22: 3D engineering drawing of the sample to be machined.....	25
Figure 23: Metallographic grinding and polishing machine.....	27
Figure 24: CoCrCuFeNi (Left) CoCrCuFeMnNi (Right)	28
Figure 25: SEM images CoCrCuFeNi.....	29
Figure 26: SEM images CoCrCuFeMnNi	29
Figure 27: XRD analysis for CoCrCuFeNi	31
Figure 28: XRD analysis for CoCrCuFeMnNi.....	31

LIST OF TABLES

Table 1: Composition of Alloy-1 (CoCrFeNiCu)	16
Table 2: Composition of Alloy-2 (CoCrFeNiMnCu).....	16

INTRODUCTION

Man has always desired to acquire materials to address modern problems without degrading. Unfortunately, this quest has had its limitations in terms of conventional alloys. Most of these alloys which are based upon one principal element with certain elements added to enhance and improve their properties. Steel is a commonly used alloy which has Fe as the principal element along with additives such as Ni, Cu, Mo etc. These alloying elements aid the common problems faced by using pure Fe in daily life applications. Corrosion is a common problem when using Fe, solved by using stainless steels having Cr as well as Ni with certain others elements used in small amounts. Similarly, there are numerous examples of such alloys being used in everyday applications.

Although conventional alloys serve the purpose but have certain drawbacks as well. Even after extensive research in this era, nothing fruitful has been achieved due to the fact that conventional alloys are confined by one or two principal elements. This has hindered the degree of freedom in terms of designing such alloy compositions that can tend to attain such morphology which meets modern requirements. Periodic table has limited number of elements and this puts a limit on the number of conventional alloys we can design.

An emerging concept in the field of material science and engineering of alloys has established the fact that there is so much more yet to be discovered. This concept of using multiple principal elements has broken the captivity of the traditional approach. Since 1995, [23] this idea of utilizing five or more than five principal elements has given birth to a new family of alloys called as 'High Entropy Alloys' which exhibit exceptional microstructures and properties. Contrary to traditional beliefs, synthesis of high-entropy alloys is possible and their analysis as well as processing is quite feasible.

1.1 High Entropy Alloys

High-entropy alloys are defined as alloys that have at least five or more principal elements having equimolar or near equimolar ratios along with minor alloying elements if any. Each element would have an atomic percentage between 5%-35%, whereas in case of any minor element less than 5%. [24] This causes the configurational entropy of the alloy to increase,

therefore stabilizing solid-solution phases more than intermetallic compounds even at high temperatures. Due to this phenomena, the synthesis of these class of alloys is quite feasible.

1.2 Four Core Effects in HEAs

The four core effects that are elaborated below have pronounced effects when it comes to HEAs and their distinctive properties. These effects govern the special microstructures and properties observed in HEAs. It should also be noted that these core effects can aid in determining the right composition for the desired application, hence these effects are important to discuss.

1.3 Entropic Stabilization

One of the core effect of adding five or more principal elements is the increase in configurational entropy, this can be understood by an example given below. Consider an alloy having one hundred A atoms which are identical. Now, as all the atoms are identical therefore only one arrangement of these atoms is possible. If one B atom replaces one A atom, the alloy would have ninety nine A atoms and one B atom. This will induce a number of arrangement of atoms this alloy can have. Similarly increasing the number of B atoms would increase the randomness of the arrangement of alloy with maximum randomness when both A and B atoms are equal. Let us add a C atom which will increase the configurational entropy even more with a maximum when all A, B and C atoms are equal. For an alloy system having five principal elements A, B, C, D and E all having equal amounts would have maximum configurational entropy. Now, according to the Gibbs free energy equation:

$$\Delta G = \Delta H - T\Delta S$$

The above equation states that Gibbs free energy is equal to difference between changes in enthalpy and product of temperature and changes in entropy. Now,

$$\Delta S_{mix} = \Delta S_{configurational} + \Delta S_{thermal}$$

Change in entropy of mix is equal to the sum of configurational as well as thermal entropy. Hence, increase in configurational entropy will cause a much more disordered system. In short, the Gibbs free energy would decrease stabilizing the solid solution phase formed by

five or more principal elements. This effect is very significant, forming the bases of high-entropy alloys.

One question remains; *how much high configurational entropy is required to form high-entropy alloy?* Well, in equimolar HEAs the configurational entropy varies from $1.61R$ for 5 number of principal elements to $2.57R$ for 13 number of principal elements ($R= 8.314 \text{ J.mol}^{-1}.\text{K}^{-1}$ which is the gas constant). [24] Lower limit for a HEA is $1.36R$, whereas the configurational entropy for conventional alloys ranges from $0.22R$ to $1.15R$ for low alloy steels and stainless steels respectively. Although any standard configurational entropy range is not defined for HEAs but $1.36R$ overlaps with that of conventional alloys therefore raising questions related to the particularity of HEAs. [24]

1.4 Sluggish Diffusion

As the lattice formed has somewhat different atoms on its sites which hinder the diffusion process in HEAs compared to conventional alloys. The vacancy formed has different energy levels due to the effect of five or more principal elements that neighbor it, whereas in conventional alloys with low concentration of solute having almost identical vacancy sites. To understand this effect, consider the diffusion of an atom to a vacancy having low energy. Now this will trap the atom and will not allow the atom to diffuse further. If the vacancy site has a higher energy, this will cause the atom to jump back to its original site hence discouraging diffusion. This sluggish effect slows down the phase transformation and diffusion kinetics in HEAs.

Tsai et al has elaborated this concept by using a seven bond model in order to calculate the effect of local energy variation upon the diffusion. The diffusion of Ni in the alloy system Co-Cr-Fe-MnNi was observed, this alloy forms a single phase F.F.C structure. The findings are very well depicted in the figure1. [25]

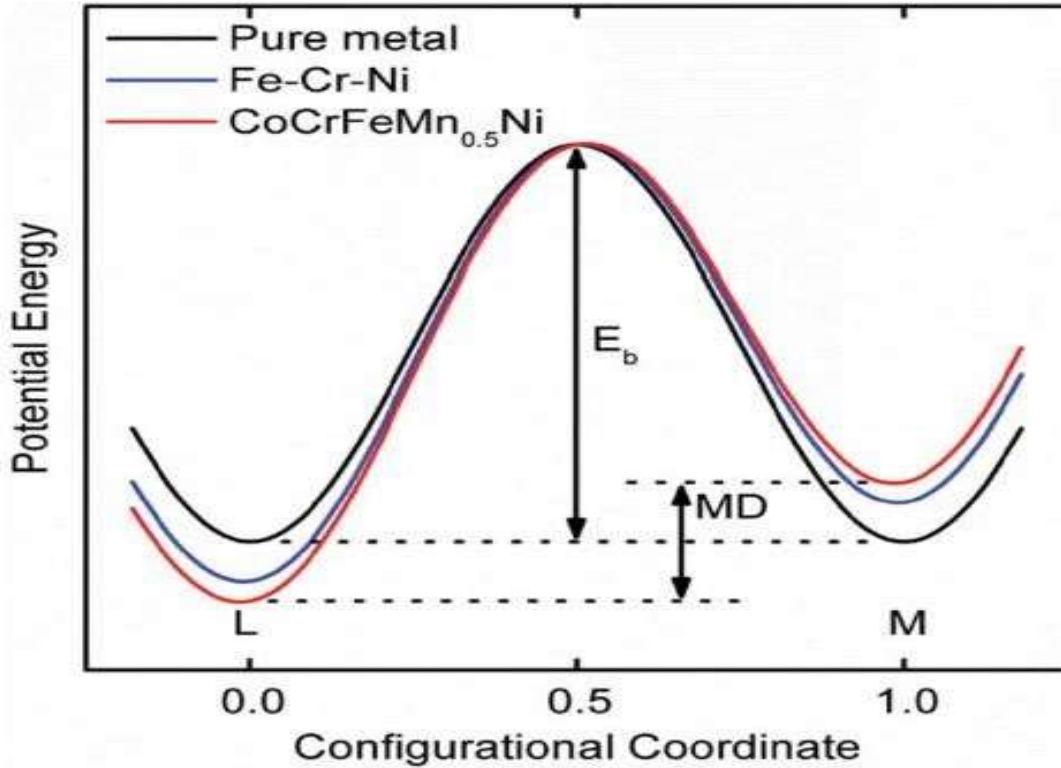


Figure 1

Figure 1 shows the potential energy difference obtained due to the diffusion of Ni atom. The mean difference (MD) due to the movement of Ni atom is zero in case of pure metals while maximum for Co-Cr-Fe-Mn-Ni. Calculated potential energy difference for the above mentioned HEA is 60.3 meV which is 50% higher than that of the Fe-Cr-Ni conventional alloy. The great difference of potential energy causes slow diffusion and longer occupation time in low energy sites. The activation energy for Co-Cr-FeMn-Ni is highest compared to conventional alloys and the experiments at melting point again result in slowest diffusion for Co-Cr-Fe-Mn-Ni alloy.

Different elements in HEAs diffuse at a different rate. Some elements diffuse slower than other, usually elements having higher melting point diffuse slower than the ones having lower melting temperatures. This results in diffusion of some elements with other

hesitating to jump from one site into another, discouraging phase transformation as the formation of another phase requires the coordinated diffusion of elements to redistribute and reach the desired composition. Also for the growth of grains, diffusion of all elements is required for the grain boundaries to migrate. In short, the slowest diffusing element becomes the rate limiting constituent hence resisting phase transformation. [25]

Due to this effect, HEAs are superior to conventional alloys in applications that require creep resistance, high temperature strength, diffusion barrier and structural stability.

1.5 Severe Lattice Distortion

Solid solution formed in HEAs have solute atoms on the lattice sites which have different sizes and electronic configuration which tends to put a strain on the lattice causing it to distort as shown in the figure 2. [23] Each element has a different bond strength and ability to form different crystal structure which distorts the lattice even more. Throughout the lattice sites, these differences vary as at least five or more solute atoms are present unlike in conventional alloys where most of the lattice sites are occupied by the solvent atoms usually.

This severe lattice distortion enhances the hardness and strength of HEAs due to solution strengthening and enables the alloy to resist the effect cause by high temperatures. Hardness observed in case of refractory bcc HEAs namely NbMo-Ta-W and V-Nb-Mo-Ta-W are 4,455 MPa (H_V) and 5,250 MPa (H_V), respectively.

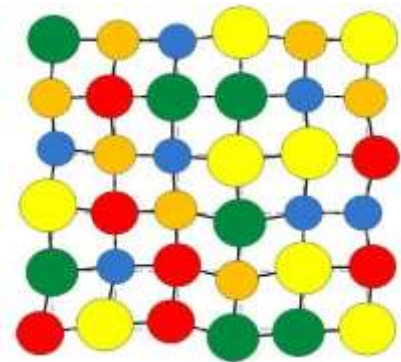


Figure 2

The latter HEA has a higher hardness due to the presence of another element forming a five equimolar alloy while the former is a four equimolar.

In HEAs, the lattice distortion caused by the thermal vibrations of elements is not as significant as the severe lattice distortion.

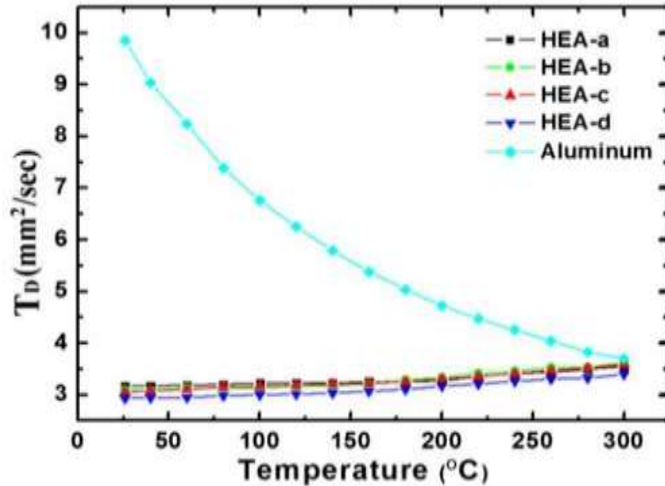


Figure 3

The results in figure 3 satisfied the above observation for HEAs. The small values of thermal diffusivity for HEAs proving insensitivity to temperature, whereas for Al we see a large value highly sensitive to temperature.

Another significant effect of severe lattice distortion is the decrease in the electrical as well as thermal properties. The above example is one of the many proofs that HEAs become insensitive to thermal and electrical effects. The scattering of electron and phonons is quite significant due to the distorted lattice of HEAs, which degrades the intensity of X-ray diffraction peaks.

1.6 Cocktail

As the words suggests, cocktail is a mix drink which has multiple ingredients added such as alcohol, fruit juice, flavors and cream. The delightful taste in the cocktail is due to the combination of multiple ingredients. Similarly, the cocktail effect is observed due to the presence of five or more principal elements in HEAs which enhance the special properties exhibited by these class of alloys. The alloy can have single or multiple phases regardless of that, the properties observed are due to the combined effect of all elements making up these phases. HEAs are more like atomic level composites and the properties come from the individual atoms as well as the mixture formed by them.

In order to verify the ‘cocktail effect’, consider the example of refractory HEAs. The four equimolar alloy system Nb-Mo-Ta-W and five equimolar alloy system V-Nb-Mo-Ta-W have melting points higher than 2600 degree Celsius, which is more than the melting

point of super alloys that are Cobalt or Nickel based. [23] The graph showing the trend is given below.

As seen from the figure 4, the softening resistance of Nb-Mo-Ta-W and V-Nb-Mo-Ta-W is much higher than Inconel 718 as well as Haynes 230. This higher resistance at elevated temperatures is due the ‘cocktail effect’ observed in HEAs.

Unlike in conventional alloys, the combined effect of all constituents should be considered as this is very critical and determines the

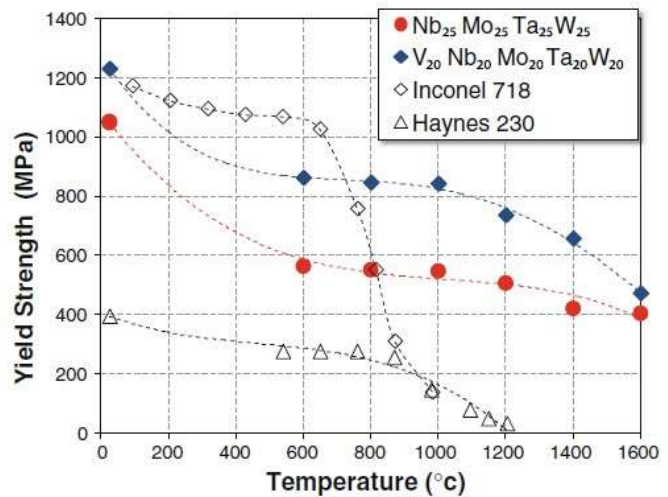


Figure 4

properties due to the addition of each element. Another example is of the ‘cocktail effect’ of Aluminum, which is considered to be a ductile and low melting element. But its properties in HEAs deviate the traditional approach, as its addition in HEA hardens the alloy.

Given in figure 5 is the trend of a HEA having Al_x-Co-Cr-Cu-Fe-Ni. As observed, the increase in at. % content of Al also increases the hardness significantly which is one of the wonders of HEAs. [23] This trend is clearly due to the phase transformation from soft FCC to hard BCC structure, also the addition of Al due its larger size and stronger binding of Al with other constituents. The above examples depict how significant the ‘cocktail effect’ is when dealing with HEAs and how the properties are influenced.

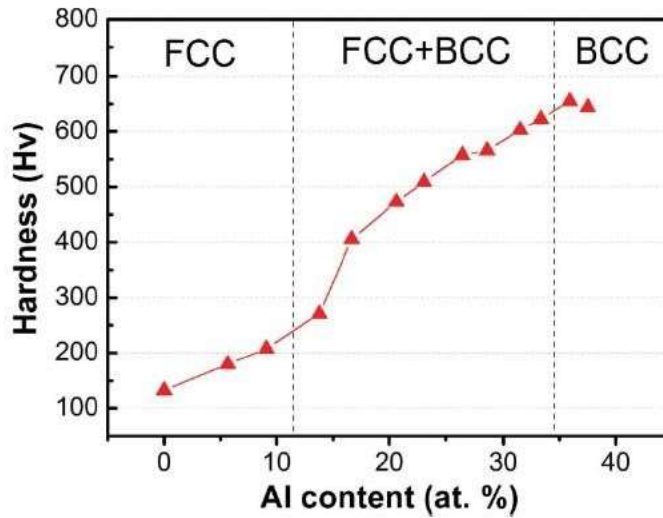


Figure 5

1.7 Properties of HEAs

1.7.1 Mechanical Properties

There is an enormous variety of the compositions of elements forming HEAs, which have broad range of mechanical properties. Hence, when discussing the mechanical properties especially hardness/strength of HEAs, it is better to discuss the properties of the major phases that are formed in case of HEAs. It is important to note that the properties depend upon the following factors:

- Hardness or strength of the formed phase in an alloy.
- The ratio of the relative phases.
- Microstructure of individual phase.

For convention, the phases formed in HEAs are divided into four categories and their trends are given below in the figure 6. [23]

Type	Examples	Typical hardness (HV)
Valence compounds	Carbides, borides, silicides	1000–4000
Intermetallic phases with non-simple structures	σ , Laves, η	650–1300
BCC and derivatives	BCC, B2, Heusler	300–700
FCC and derivatives	FCC, L1 ₂ , L1 ₀	100–300

Figure 6

Valence compounds have highest values as they are ceramics due to strong covalent bonding. The second non-simple structures hinder dislocation movements and hence have

hardness rating up to 1300 *HV*, then comes the BCC which have strong directional bonding and are more closely packed compared to FCC. The fact that these ranges are general should be considered as exceptions have also been reported. For instance, refractory HEAs which mainly have elements such as Cr, Hf, Ta, Zr, Nb, V and W. These HEAs form BCC structure which has strength 900-1350 MPa. [23] Also, plastic fracture strain for most alloys is below 5% whereas some alloys can be compressed to 50% without fracture. [23]

1.7.2 Wear and Fatigue Properties

HEAs exhibit exceptional wear resistance under both adhesive and abrasive conditions. Trends of multiple HEAs along with conventional alloys have been reported in figure 7 depicting the wear resistance of HEAs. [23]

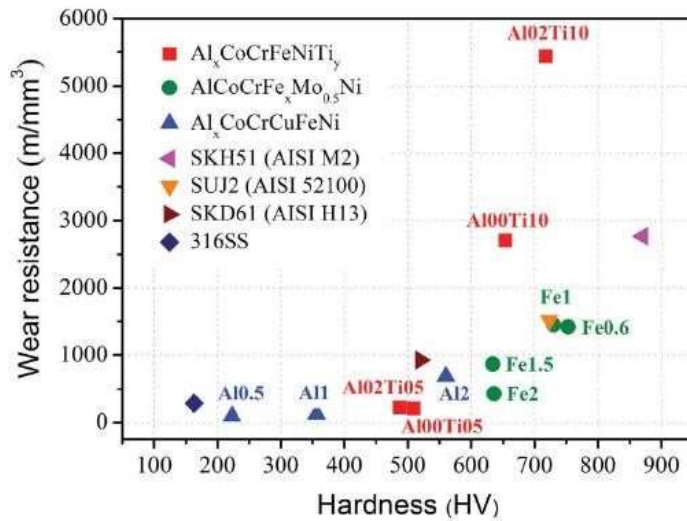


Figure 7

Also, another exceptional example of the alloy Al_{0.3}-Cr-Fe_{1.5}-Mn-Ni_{0.5} which has amazing surface hardening property increasing wear resistance up to 50% approximately with bending strain reduced by only 2%. Not just this, the alloy Al_{0.5}-Cr-Fe-Mn-Ni has fatigue properties which are superior to most Ti or Zr based conventional alloys. This HEA shows high endurance to stress ranging from 540 MPa to 945 MPa. [23]

1.7.3 Elevated Temperature Properties

Most of the HEAs exhibit exceptional properties at elevated temperatures due to the sluggish diffusion effect compared to conventional alloys. Figure 8 gives the exceptional hot hardness of HEAs which is even higher than Inconel 718 [23]

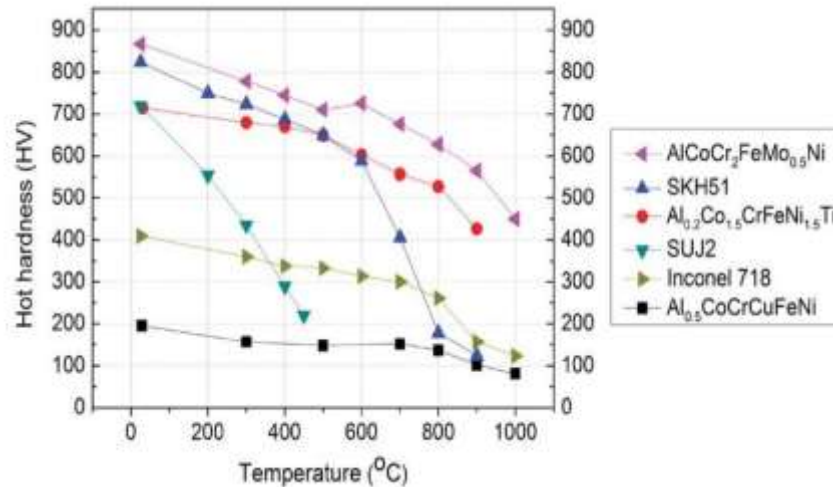


Figure 8

1.7.4 Corrosion Properties

It is not an overstatement that HEAs exhibit corrosion resistance as well as resistance to pitting even higher than 304 SS and 304L SS when analyzed in solutions such as NaCl and H₂SO₄. It is to be noted that some HEAs suffer remarkable corrosion. For instance, Co-Cr-Fe-Ni has better corrosion properties than 304 SS but when Cu is added to the system, the alloy experiences severe galvanic corrosion and corrosion resistance is significantly decreased. Addition of Al also degrades the pitting resistance of the alloy system. Also, Mo added aids corrosion resistance as it forms a broad passivation region. To summarize the corrosion properties, it is to be noted that different HEAs behave differently in different environments and while designing a HEA, the working environment of the alloy should be considered. [23]

1.8 Potential Applications

HEAs can have numerous applications depending upon the designed alloy system, some of the major potential applications of HEAs are:

1.8.1 Thermal Barrier Coatings

Nano precipitated structures obtained in HEAs even in as-cast state unlike in conventional alloys and the sluggish diffusion effect creates HEAs ideal for applications that require resistance to heat as well as electrical properties.

Material		HE alloy A	HE alloy B	SKD61
Thermal conductivity (W/mK)	Bulk	7.94	6.69	28
	Coating	3.24	3.14	

Figure 9

As seen in figure 9, [24] the thermal coating of HE alloy A and B is way below that of commercial hot mold steel SKD61.

1.8.2 HardFacing Applications

HEAs are highly recommended for hardfacing applications as they have high wear resistance, high hardness, high corrosion resistance and high temperature softening resistance compared to conventional alloys. This makes HEAs suitable for applications where hardfacing technology can be used to protect machine components and tools. [26]

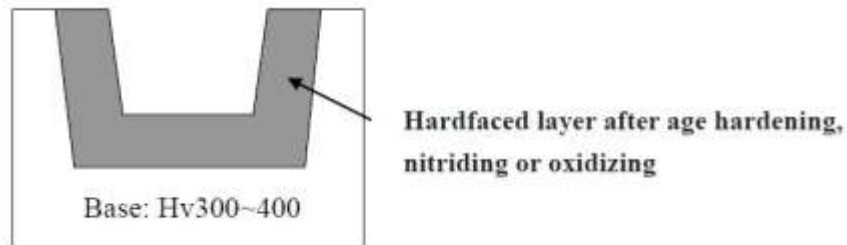


Figure 10

Also, HEAs can be used where traditional alloys cannot withstand high friction and wear away. Figure 11 depicts the trend of wear resistance observed in HEAs compared to conventional alloys. [26]

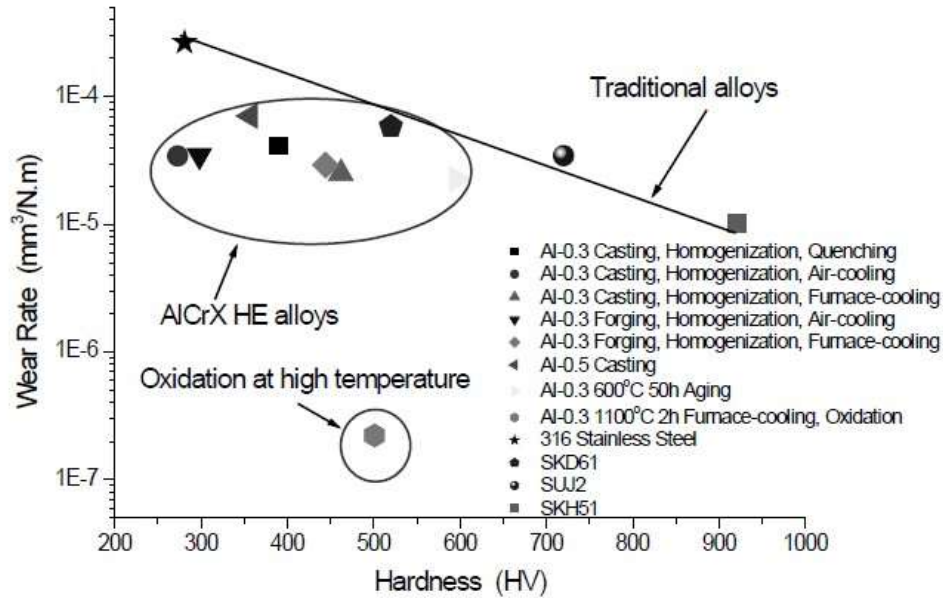


Figure 11

1.8.3 Antibacterial and Electromagnetic Interference Shielding Coatings

The following table shows the antibacterial properties of HEAs as they have certain significant properties in the field of biochemistry. [26]

Bacterium name	Colony-forming unit of comparison group after 24h	Colony-forming unit of sample group after 24h	Antimicrobial activity	Antibacterial rate (%)
S. aureus	2.1×10^6	< 10	5.32	>99.999
Escherichia coli	1.1×10^6	< 10	5.04	>99.999
Klebsiella pneumoniae	1.6×10^6	< 10	5.20	>99.999
Pseudomonas aeruginosa	1.9×10^7	< 10	6.28	>99.9999

Figure 12

Figure 12 showing HEA coatings which tend to show inhibition to formation of colony. The antibacterial rate for all types of bacteria are greater than 99.9% hence depicting antibacterial abilities of HEAs.

The electromagnetic interference (EMI) is a common issue where HEAs can serve the purpose. The shielding effect provided by HEAs increases with increasing frequencies as shown in figure 13. [26]

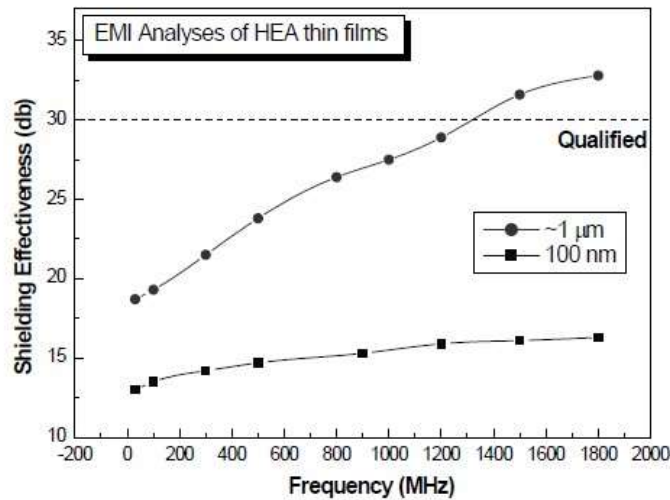


Figure 13

Shielding effect of multiple thickness HEA coatings as a function of frequency. A HEA coating having 1 micrometer thickness at higher frequencies qualifies for the standard shielding required for commercial applications. Hence through designing the right HEA, we can use them to coat electronic components with additional properties such as anti-oxidation, wear resistance and anti-bacteria and EMI shielding.

There are numerous other applications where HEAs surpass conventional alloys by exhibiting extraordinary properties. Through designing the right alloy system, we can utilize them to address the shortcomings of conventional alloys. HEAs can be used for commercial applications such as thermal barriers, wear-resistant materials, graded materials, hard metals, anti-bacterial and EMI shielding coatings. HEAs have so many potential applications which can be commercialized through proper research and development.

CHAPTER 2

LITERATURE REVIEW

To start working on High Entropy Alloy we first needed to understand their basic principles that make these class of materials unique. Foremost helpful was the book “High Entropy Alloys by BS Murty, J.W. Yeh and Ranganathan” through which we were able to grasp the basics and behavior of High Entropy Alloy. The book discussed the history, development and milestones in research. This was the framework in understanding the properties that that these materials exhibit. Given the wide range of possible alloy compositions and the even greater spectrum of functional properties such as corrosion resistance, Irradiation resistance, catalytic properties, gas storage, magnetic properties, thermal properties, electrical properties [1] we were presented with an open choice to guide our research.

To design our first High Entropy Alloy samples, we studied existing HEA systems and techniques to develop our own systems. Such techniques included both combinatorial and computational methods [2]. Combinatorial methods are more hit and trial based and unfortunately are time and material consuming. On the other hand, have computational techniques that rely on mathematics and simulations to accurately predict phases. These techniques use the available thermodynamic data and mixing entropies of metals to calculate phases and the relative amounts of elements present in each.

Major metallic elements	Minor metallic elements	Minor non-metallic elements
Li, Be, Mg, Al, Sc, Ti, V, Cr, Fe, Co, Ni, Cu, Zn, Y, Zr, Nb, Mo, Sm, Eu, Au, Gd, Tb, Rh, Pb, Pd, Ag, Hf, Ta, W, Pt, Nd	Li, Be, Mg, Al, Sc, Ti, V, Cr, Fe, Co, Ni, Cu, Zn, Ga, Ge, Sn, Sb, Y, Zr, Nb, Mo, Ru, Rh, Pb, Bi, Pd, Ag, Hf, Ta, W, Pt, Au, La, Ce, Pr, Nd, Sm, Eu, Gd, Tb	C, B, Si, P, S, O, N

Figure 14 List of all possible elements that can be used in HEAs [5]

Some of these computational techniques include CALPHAD [3], AIMD simulations, DFT calculations [4], Taguchi method [5] and others. Thermo-Calc (Thermo-Calc Software, Stockholm, Sweden) is another computational tool used when direct experimentation is expensive, inconvenient or time consuming. However, the major issue with computational techniques at the moment is that most of them are database dependent with large majority of data consisting for binary alloys [2]. High Entropy Alloy have not yet had a notable representation in literature yet but continued work is underway. Also simulations tend to be time consuming and difficult to design [4].

Employing knowledge of material science is the more common method for development of HEAs. However, in method is complicated as it requires prior accurate understanding of crystal structures, electro-negativities, valence electrons, densities, atomic sizes as a well as concepts including thermodynamics, kinetics, microstructures and other fundamentals of alloy design and material science. This is a more popular approach taken by researchers as it allows much greater degree of freedom relating to control over compositions [2]. Such a crude route is only becoming more wide spread as more data on HEA systems is being reported.

After deciding upon the alloy composition, the next step is to actually produce or manufacture the alloy. This can be done by resistance melting, induction melting, arc melting, plasma spraying, powder metallurgy and mechanical alloying [7]. Most of these techniques require an Argon atmosphere but do differ in the type of crystal structure that could result ignoring post treatments [5]. Each have their own merits and demerits as well as degree of ease of use.

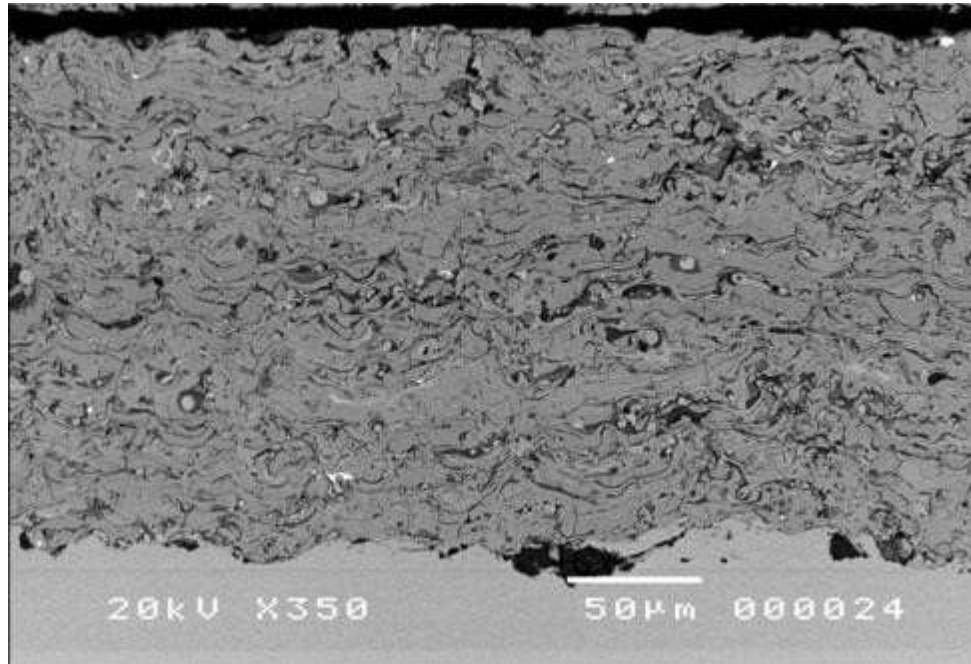


Figure 15: Structure of AlCoCrFeNiSiTi alloy plasma sprayed on 304 Stainless Steel [2]

Mechanical Alloying involves using metallic powders and milling them at high speeds. The result is formation of two terminal phases namely amorphous and another solid solution. To stop the powders from conglomerating the powders can be cooled by liquid nitrogen, milling at normal RT temperature is then continued later [8] after which sintering is done performed. This technique was first introduced for oxide dispersion strengthened NI bas super alloys by Benjamin and his colleagues but BS Murty and his team were the first to develop Nano-crystalline AlFeTiCrZnCu equi-atomic HEA using mechanical alloying [1]. The Nano-crystalline alloy achieved showed promising thermal stability and mechanical properties. Nano-crystalline structure are subject to grain growth hence are sintered in spark plasma sintering setup to mitigate grain growth

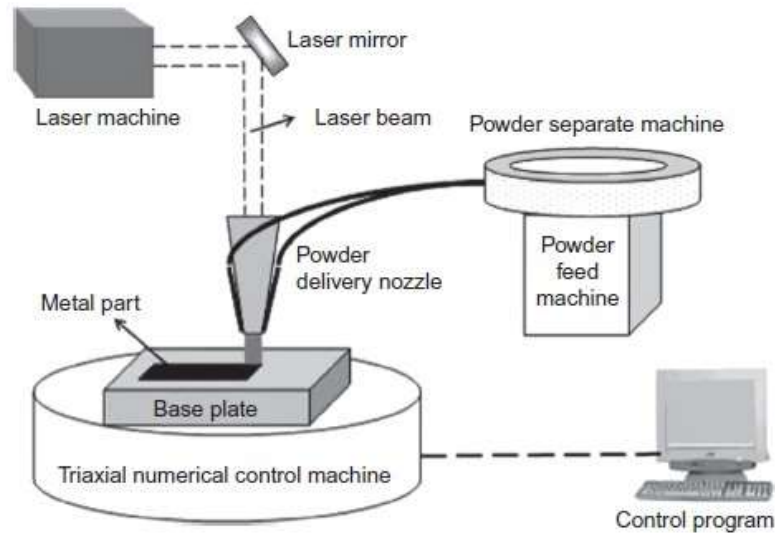


Figure 16: Schematic of LENS Technique [1]

Additive technology has also been employed for use in HEA manufacturing. One of these is the Laser-engineered Net Shaping Technique. It deposited powdered metal that is heated and melted onto a substrate by use of a high energy laser [9]. One advantage of this technique is the close control over composition as gradients can be introduced through the dimensions of the material to form Gradient HEAs. HEA rods with varying compositions have already been developed [1]. The desired shape and dimensions can be achieved as the table as two dimensions degree of freedom allowing complicated construction.

However, the most widespread route for manufacturing High Entropy Alloys is the Use of Arc Melting and Casting. The popularity of this technique can be derived from the fact that 75% of research quoted till 2013 used arc melting as their manufacturing technique [1]. The advantage of arc melting comes in the form of the extremely high temperatures that can be achieved around 3000 Degree Celsius. However, this proves to be a double-edged sword as due to the high temperatures attainable the low melting metals can just as easily become vaporized which can prove to be detrimental to the composition of the alloy.

Since our aim is for development and characterization of High Entropy Alloy foam we looked into the techniques to introduce porosity into our metal alloy. Although porosity may already be present in a cast metal but that is a defect and not a desired property. Our

aim is to devise a method to introduce uniform and distributed porosity. Powder Metallurgy offers a route in which porosity causing agents can be introduced. These volatile agents during sintering remove themselves from the metal matrix to leave behind macro sized pores [10]. Other possible techniques included fiber metallurgy, electro-chemical deposition, slip casting [10] or use of selective laser melting which has been successful in case of 304 stainless steel [11]. Selective dealloying is also another method which requires chemical agents to remove elemental components from alloy matrix [12][16].

We have observed that the mechanical properties of HEA systems have been thoroughly discussed. There is abundant data available their phases, mixing entropies, and microstructures. However, discussion about their performance in electrical application are few and far in between and the work of electrical properties for HEA foams even fewer. This leaves an entire direction of research in HEA foam for electrical application open for study. To look into characterization of HEA foams for their properties we looked into the characterization used for traditional metallic foams. Some promising findings have already been reported as for use of porous HEAs as electrode for super-capacitors.

Supercapacitors are one of the heavily researched electrical components of the decade, due to their ability to offer power almost instantly due fast charge and discharge cycles and low degradation over time compared to traditional batteries they have shown promise in energy application especially in replacing batteries for use in high performance electric vehicles [17][18]. Characterization techniques include cyclic voltmetry, charge Discharge cycle measurements, Lifecycle Testing, high precision thermocouple monitoring [13], DoD, retention for internal resistance and capacitance [14], determination of acceleration factor and retention, Electrochemical Impedance Spectroscopy (EIS)[16], voltage and thermal dependence [15][18].

Multiple materials have been employed in use for supercapacitor electrodes ranging from Metal Organic Frameworks *MOFs*, ternary metal oxides, MnO₂ nanosheets to CNTs all having varying different properties and structures. The common all of them care is porosity as it allows the active electrolyte to penetrate the material [18]. However, Kyeongho Kong and his colleagues developed a nano-porous AlCoCrFeNi foam and tested its electrical

performance for supercapacitor application he found that the performance was similar to previously mentioned materials [16].

EXPERIMENTAL PROCEDURES

3.1 Alloy Design

Once we had decided on the composition the next step was to garner the parent materials in the equimolar ratios. Since, every element has a different molar mass. Therefore, we cannot simply garner them in equal weights. Hence, we have to first convert their equi-atomic ratios to corresponding weight ratios. The calculations were performed by using Excel. Two high entropy alloys of different compositions were to be made. Hence alloy designing was performed for two different samples with each of them having a total weight of 10 grams.

Table 1: Composition of Alloy-1 (CoCrFeNiCu)

Element	at%	wt%	Weight (in grams)
Co	20	20.39	2.039
Cr	20	17.99	1.799
Fe	20	19.32	1.932
Ni	20	20.31	2.031
Cu	20	21.99	2.199
Total	100	100	10

Table 2: Composition of Alloy-2 (CoCrFeNiMnCu)

Element	at%	wt%	Weight (in grams)
Cr	16.03	14.48	1.448
Mn	16.03	15.30	1.530
Co	16.03	16.41	1.641
Fe	16.03	15.55	1.555

Ni	16.03	16.34	1.634
Total	100	100	10

3.2 Cutting and Weighing of the Materials

After alloy designing was complete the next step to cut the metal chunks and weigh them as per the alloy design. Conventional metal pliers were used for cutting the metal chunks and a high precision analytical weighing balance was used for weighing the metals as per the alloy design. Extreme care and caution were observed to ensure that the weight ratios are not disturbed.



Figure 17: Analytical weighing balance

3.3 Washing and cleaning

Then the metals were washed with methyl ethanol and placed in a sonification bath. This was done to ensure that dust and other foreign particles are removed at this stage and don't



Figure 18: Sonication Bath

become a part of the alloy formation process.

3.4 Arc Melting

For arc melting the parent elements are to be placed in the arc furnace in such a way that the metal with the highest melting point is placed at the top layer and the preceding layer is of the metal with the next highest melting point and so on. This layer by layer approach is repeated such that the bottom layer is of the metal with the lowest melting point. The significance of this is that the heat from the arc is first transferred to the metals with higher melting points and later it reaches to the metals with lower melting points. Therefore, all the metals melt at approximately the same time. So, it will be easier for us to achieve homogenous mixing. Therefore, we placed Chromium at the top layer and Copper was placed at the bottom layer.



Figure 19: Layer by layer stacking of parent metals (left) closing the door of melting chamber and vacuum generation (right)

After stacking the parent metals layer by layer, the door of the furnace was closed and vacuum was generated. Then the protective shield was brought up and the arc was initiated. Once the heat generated from the arc entered the metal pile, fumes started to appear. These fumes were of the metal with the highest melting point i.e. Chromium. The arc was rotated in the melting chamber for a small period of time and then it was brought to rest and was turned off in order to avoid the overheating of the furnace. Then the metal pile was inverted and the arc was then again ignited and rotated. This process was repeated 5 times to ensure uniform melting of the metals and their homogenous mixing.

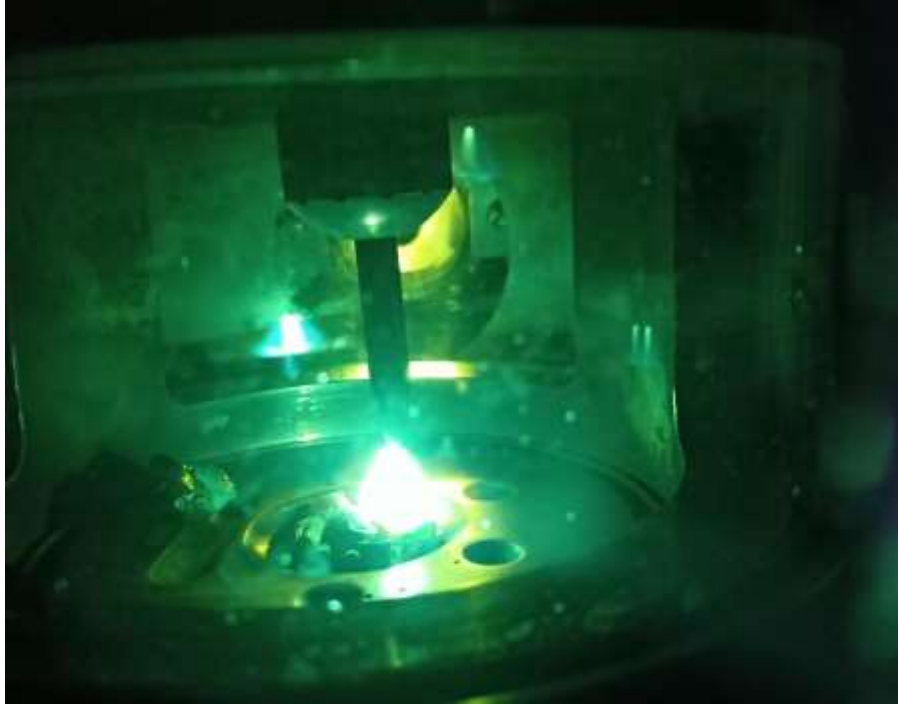


Figure 20: Protective shield is up and arc is generated

Afterwards, the furnace was turned off and the newly formed alloy was left inside the melting chamber for a while so that it completely cooled off.

3.5 Machining

Once the alloy was formed, the next step was its characterization and testing for relevant studies. In order to do that we had to first extract standard samples from the solid chunk of the formed alloy.

For this purpose, the engineering drawing for the samples of rectangular shape was designed by using AutoCAD. The samples had the dimensions of $7 \times 2 \times 2$ mm and was manufactured by EDM cutting.

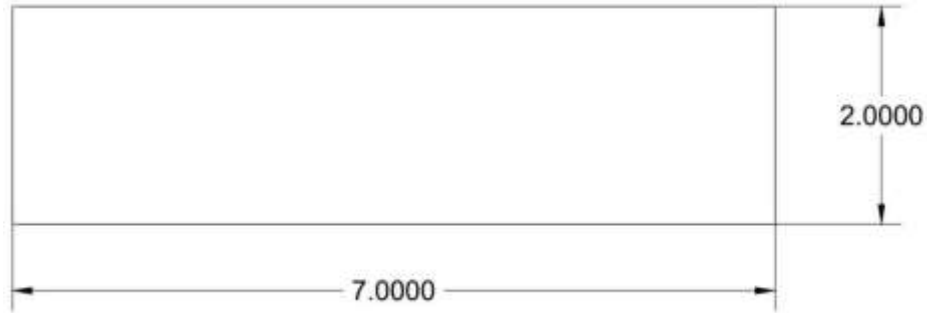


Figure 21: 2D engineering drawing of the sample to be machined

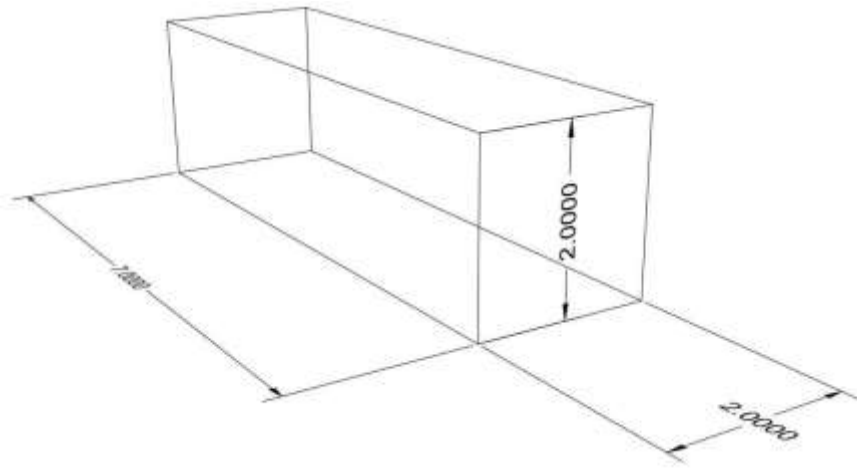


Figure 22: 3D engineering drawing of the sample to be machined

3.6 XRD

For characterization of the High Entropy Alloy, we used X-ray Diffraction (XRD). Its purpose was to confirm that each parent element was present in the formed High Entropy Alloy. And that each parent element was properly distributed across various plane geometries.

The testing parameters for the XRD of our samples included a scan time of 1 hour and scan angles from 20° to 90°.

3.7 SEM

The next step in characterization involved studying our HEA samples under a Scanning Electron Microscope (SEM). Its purpose was to verify the phase formation from parent elements. We also intended to study the grain structure.

3.7.1 Sample Preparation

In order to perform SEM on our high entropy alloy, we first had to perform various operations on our samples to make them suitable for studying under SEM.

3.7.2 Metallographic Mounting

The first step involved mounting our HEA samples on a cylindrical support of Bakelite. We utilized hydraulic pressing for this purpose. The significance of this step is that it allows us to easily perform the metallographic operations in the subsequent stages.

3.7.3 Grinding

After we had mounted the HEA sample, the next step was to perform grinding. We used SiC Abrasive Paper for this purpose. The significance of grinding is that it removes any scratches from the area of interest.

3.7.4 Polishing

We then performed polishing of our samples. The significance of polishing is that it removes dust and other foreign particles from the area of interest. For polishing of our samples, we used a alumina solution which had an alumina to water ratio of 3:1 and the size of alumina particles was 1 micrometer.



Figure 23: Metallographic grinding and polishing machine

3.7.5 Etching

In the end we performed etching of our samples so that the grain boundaries and other features were highlighted and we can easily study them under SEM. For this purpose, we used Aqua Regia which is a mixture of HCL and HNO₃ at the ratio of 4:1. Once our samples were prepared, we then studied them under SEM.

RESULTS AND DISCUSSION

4.1 Optical microscopy

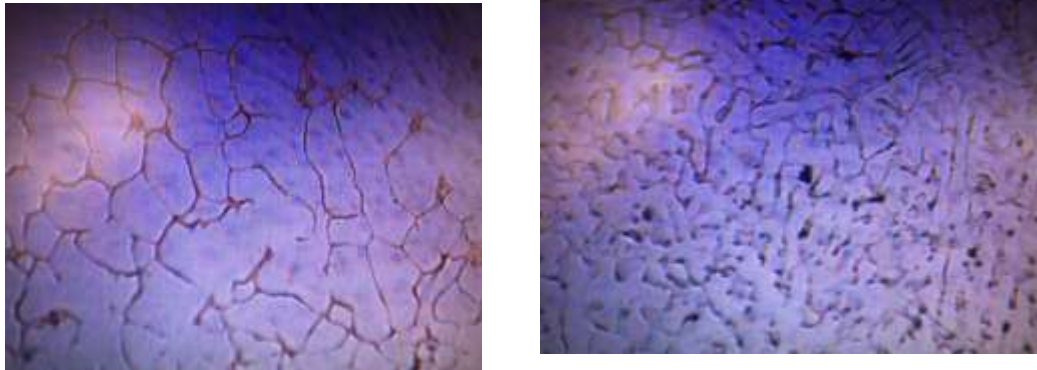
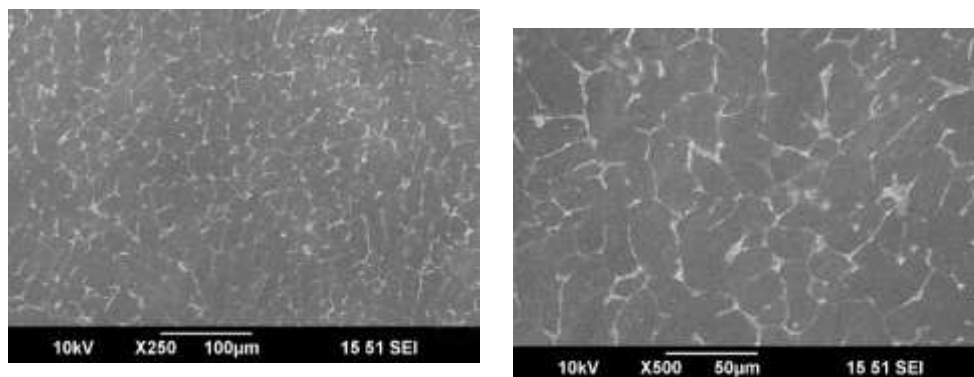


Figure 24: CoCrCuFeNi (Left) CoCrCuFeMnNi (Right)

We can see by the results procured from optical microscopy at a magnification of 80X that the structures for both CoCrCuFeNi and CoCrCuFeMnNi are significantly different from each other in terms of morphology. CoCrCuFeNi displays a widely branched dendritic structure whereas in CoCrCuFeMnNi visually demonstrates a more non-compliant structure to a dendritic structure.

4.2 Scanning Electron Microscopy



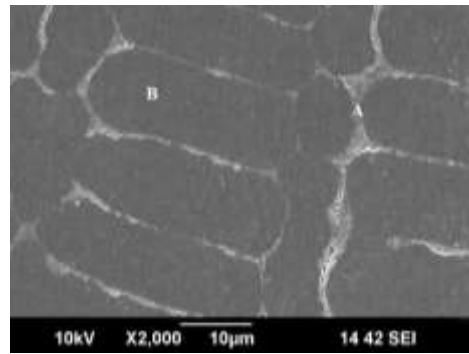
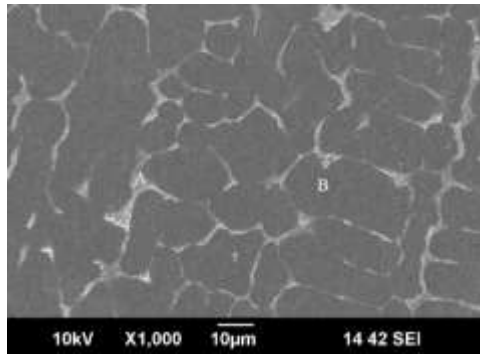


Figure 25: SEM im

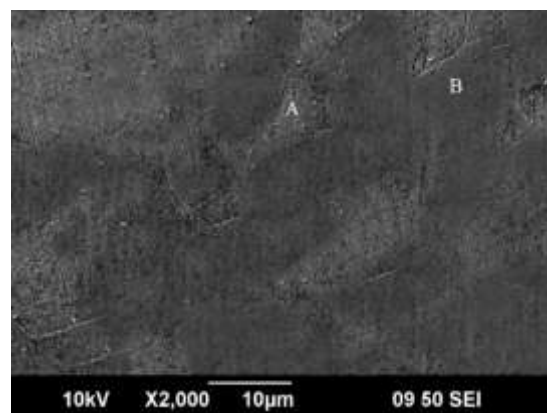
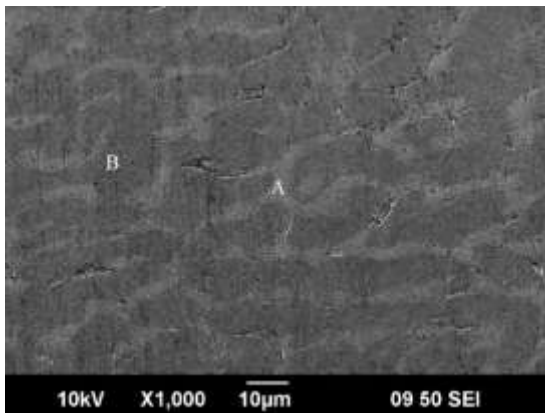
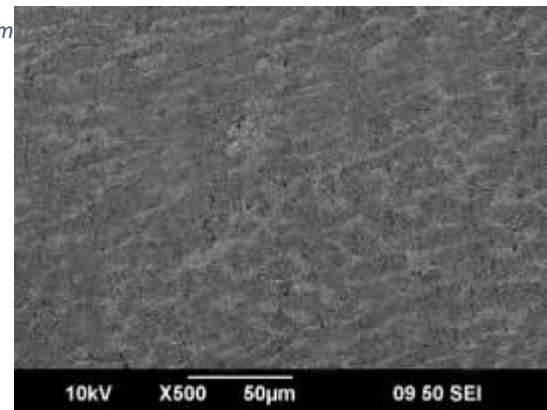
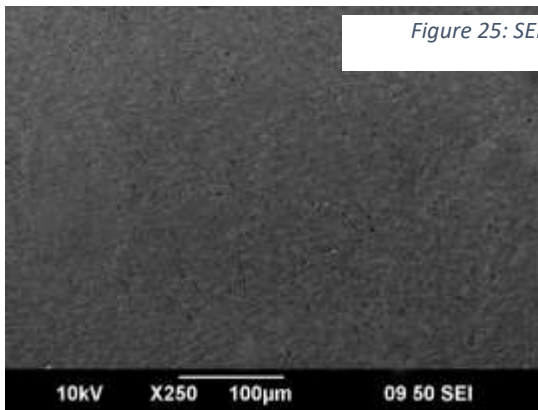


Figure 26: SEM images CoCrCuFeMnNi

Analyzing the SEM images for CoCrCuFeNi consider the images at a magnification of 1000X and 2000X. We can see two distinct regions. These two regions are not only differentiated on basis of contrast but also on basis of composition. The region labeled as A is a Cu rich region whereas the other labeled region namely region B is a Cu lean region. We can see that the Cu rich phase is uniformly branched throughout the sample with extended veins. On further analysis of the image using ImageJ software we measured the thickness of this phase as present in the images. For that a scale was set in software and the width was conservatively measured at multiple points and the collective data was then averaged to show that the average thickness is 2.27 microns. Now considering the SEM images from nonequimolar CoCrCuFeMnNi we can see that a much similar two phase morphology is present just as in equimolar CoCrCuFeNi. The two Cu rich and Cu lean regions are labeled as region A and B respectively. Using the same procedure to measure the thickness of the Cu rich phase branches in the previous sample the branch thickness was measured to be 3.47 microns. Even on visually comparing the SEM images for both samples we can see that CoCrCuFeMnNi has a more uniformly branched morphology with a higher vein thickness. The presence of these two regions is in accordance to reported data on CoCrCuFeMnNi and CoCrCuFeNi HEA classes. The interdendritic phase segregation we see on both samples is due to difference in volume fractions, liquid phase immiscibility, low solidification point of Cu as well as the average solidification temperatures of the constituents resulting in a Cu rich and deficient region [27].

4.3 XRD

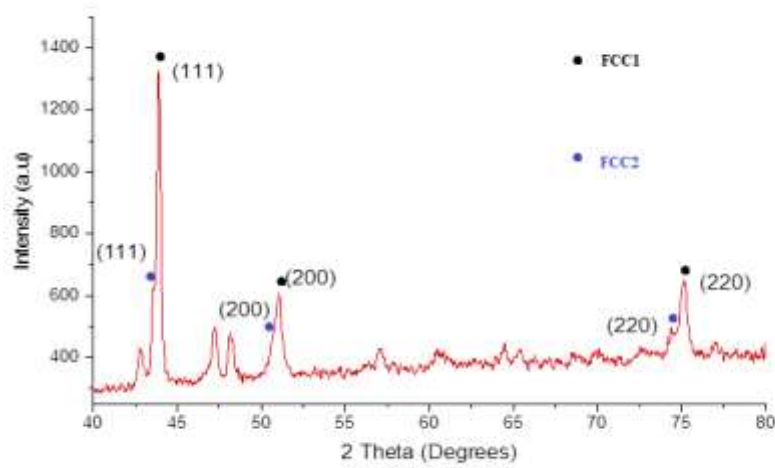


Figure 27: XRD analysis for CoCrCuFeNi

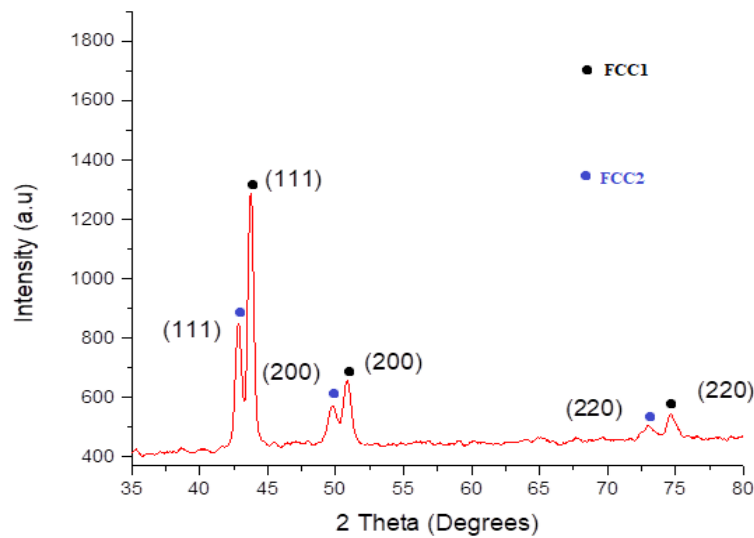


Figure 28: XRD analysis for CoCrCuFeMnNi

The X-ray diffraction data further supports our findings from the SEM images as we can now also see that two distinct phases are present on the diffraction graphs for both CoCrCuFeNi and CoCrCuFeMnNi. Taking into focus the results for CoCrCuFeNi can see that the peaks exist for planes (111), (200) and (220). This correlates the structure being FCC for both phases. The peaks are further labeled as FCC1 and FCC2. FCC1 is the primary

FCC phase and FCC2 is the secondary FCC phase. FCC1 are the peaks generated by the High entropy matrix whereas FCC2 are due to the Cu rich phase formed due to interdendritic phase segregation which is true for both CoCrCuFeNi and CoCrCuFeMnNi. The position and existence of these peaks are supported by literature findings and this similar trend is found true for HEA families with similar constituent elements [27] [28]. This phase segregation occurred during solidification stage of the as cast alloy. For CoCrCuFeNi the diffraction angles for FCC1 are present at 43.88°, 51.05° and 75.21° whereas for FCC2 the diffractions angles are at 43.54°, 51° and 74.5° moving left to right. For CoCrCuFeMnNi the diffraction angles for FCC1 are present at 43.69°, 50.86° and 74.53° whereas for FCC2 the diffractions angles are at 42.7°, 49.73° and 73.1° moving left to right.

4.4 Weight loss measurement

CoCrCuFeMnNi provided us with more consistence data and had a highly branched structure with the Cu rich phase. It also had a greater vein thickness compared to CoCrCuFeNi. Hence we decided to create a porous structure by removing the Cu rich phase present due to interdendritic phase segregation. A solution was prepared consisting of components that would have high affinity to the Cu rich phase and can slowly remove it through electrochemical phase dissolution. The two machined samples were cleaned and placed in the solution for 24hours. After which the samples were removed from the solution, cleaned, dried and measured for weight loss. The two samples were measured pre de-alloying to be 202g and 193g. Post de-alloying the samples weighed 193.92g and 179.49g with averaged percentage weight loss accounting to 10.5%. The procedure we followed for selective phase dissolution for porous HEAs is documented in literature [16].

CONCLUSION

Since research in conventional alloys has reached its limit, it is important to investigate and exploit the properties of High-Entropy Alloys and look for the potential applications in which HEAs can replace conventional alloys due to their extraordinary properties.

The SEM imaging of the two alloy systems CoCrCuFeNi and CoCrCuFeMnNi shows two different morphologies. From the SEM analysis, we conclude that we get two regions; Cu rich and lean. This two phase region is evident of the fact that High-Entropy system was successfully developed. Upon comparing the SEM images, we see that the presence of these two regions is in accordance to reported data on CoCrCuFeMnNi and CoCrCuFeNi HEA classes.

X-Ray diffraction analysis was done on both the samples and conclusions drawn from that are that both the graphs of the two alloy systems depict the presence of FCC1 and FCC2. Literature review enables us to conclude that FCC1 peaks are formed due to the presence of high-entropy mix phase whereas the peaks which are labeled as FCC2 are due to the Cu rich phase formed due to inter-dendritic phase segregation which is true for both CoCrCuFeNi and CoCrCuFeMnNi.

The weight loss measurements provide us the bases to conclude the formation of a porous structure after a 10.5% weight loss through selective phase dissolution of the Cu rich phase. The results above allow us to form certain conclusions about the formation of a two phase high-entropy porous alloy system and these findings have solid bases and supporting literature as well.

CoCrCuFeMnNi and CoCrCuFeNi high-entropy alloy systems we developed belong to the class of HEAs which are found to have excellent electrochemical properties and hence we believe that these alloy systems can exhibit extraordinary electrical properties and show great performance in certain enabling them to be used in certain potential applications such as electrodes for super capacitors. As these alloy systems due to the four core effects of HEAs mentioned in the introduction can form oxides which are a lot more conductive than conventional alloy oxides which have one or two principal alloying element. Hence the blend of high specific surface area due to the porous structure and conductive oxides can make these alloy systems excellent super capacitors. Also the porosity can play an important role in twisting the properties such as deformability and specific surface area hence enhancing the spectrum of potential applications. A porous structure can also be used in areas where lightweight materials can create a huge impact on the performance. In short, there is a need to study HEAs as well as investigate the unusual properties exhibited by these alloy systems and look for possible replacements, where conventional alloys lack performance and have drawbacks hence allowing us to make more efficient systems.

References

- [1] High Entropy Alloys, BS Murty, J.W. Yeh, S.Ranganathan
- [2] Alloy Design Strategies and Future trends in High Entropy Alloys, Jien-Wei Yeh
- [3] Current and emerging practices of CALPHAD toward the development of high entropy alloys and complex concentrated alloys
- [4] High-entropy alloy, challenges and prospects
- [5] High Entropy Alloys Development and Applications, Steadyman Chikumba and Veeredhi Vasudeva Rao
- [6] Phase Formation in Equiatomic High Entropy Alloys:CALPHAD Approach and Experimental Studies
- [7] An assessment on the future development of high-entropy alloys, Z. P. Lu, H. Wang, M. W. Chen, I. Baker, J. W. Yeh and C. T. Liu
- [8] Nanostructured high entropy alloys with multiple principal elements novel alloy design concepts and outcomes, Jien-Wei Yeh, Swe-kai Chen, Su-Jien Lin, Jon-Yiew Gan, Tsung-Shune Chin, Tao-Tsung Shun, Chun-Huei Tsau and Shou-Yi Chang.
- [9] Additive Manufacturing of Metals: A Review E. Herderick
- [10] Porous Metals, Vladimir Shapovalov
- [11] Development of porous 316L stainless steel with novel structures by selective laser melting, Z. Y. Wang, Y. F. Shen and D. D. Gu
- [12] Nanoporous Metals by Dealloying Multicomponent Metallic Glasses. By Jinshan Yu, Yi Ding, Caixia Xu, Kihisa Inoue, Toshio Sakura, Mingwei Chen
- [13] Cycle Testing of Supercapacitors for Long-Life Robust Applications, Donal B. Murray, Member, IEEE, and John G. Hayes, Member, IEEE
- [14] Accelerated Charge–Discharge Cycling Test and Cycle Life Prediction Model for Supercapacitors in Alternative Battery Applications, By Masatoshi Uno, Member, IEEE, and Koji Tanaka
- [15] Frequency, thermal and voltage supercapacitor characterization and modeling. By F. Rafika, H. Gualous, R. Gallay, A. Crausaz, A. Berthon
- [16] Nanoporous structure synthesized by selective phase dissolution of AlCoCrFeNi high entropy alloy and its electrochemical properties as supercapacitor electrode, By Kyeongho Kong, Jaeik Hyun, Yongjoo Kim, Wontae Kim, Dohyang Kim
- [17] Review of characterization methods for supercapacitor modeling, By Nathalie Devillers, Samir Jemei, Marie-Cécile Péra, Daniel Bienaimé, Frédéric Gustin
- [18] Super capacitors, By Joanna Conder, Krzysztof Fic, Camelia Matei Ghimbeu

- [19] Significant Effect of Pore Sizes on Energy Storage in Nanoporous Carbon Supercapacitors Christine Young, Jianjian Lin, Jie Wang, Bing Ding, Xiaogang Zhang, Saad M. Alshehri, Tansir Ahamad, Rahul R. Salunkhe, Shahriar A. Hossain, Junayet Hossain Khan, Yusuke Ide, Jeonghun Kim, Joel Henzie, Kevin C.-W. Wu, Naoya Kobayashi and Yusuke Yamauchi
- [20] Microstructures and thermodynamic properties of high-entropy alloys CoCrCuFeNi. By Bo Wu, Zheyu Xie, Jinchang Huang, Jinwei Lin, Yixu Yang, Linqiao Jiang, Jianglin Huang, Guoxin Ye, Chunfeng Zhao, Shangjin Yang, Baisheng Sa
- [21] Semi-solid processing of the CoCrCuFeNi high entropy alloy. By Rogal
- [22] Effect of Co content on the phase transition and magnetic properties of Co_xCrCuFeMnNi high-entropy alloy powders. By Rui-Feng Zhao, Bo Ren, Guo-Peng Zhang, Zhong-Xia Liu, Jian-jian Zhang
- [23] Alloy Design Strategies and Future Trends in High-Entropy Alloys, JIEN-WEI YEH
- [24] Exploration and Development of High Entropy Alloys for Structural Applications, Daniel B. Miracle *, Jonathan D. Miller, Oleg N. Senkov, Christopher Woodward, Michael D. Uchic and Jaimie Tiley
- [25] High-Entropy Alloys: A Critical Review, Ming-Hung Tsai & Jien-Wei Yeh
- [26] INDUSTRIAL DEVELOPMENT OF HIGH-ENTROPY ALLOYS, Wei-Hong WU, Chih-Chao YANG, and Jien-Wei YEH
- [27] Microstructural stability and mechanical properties of equiatomic CoCrCuFeNi, CrCuFeMnNi, CoCrCuFeMn alloys Seung Min Oh, Sun Ig Hong Department of Materials Science and Engineering, Chungnam National University, Daejeon, 34134, South Korea
- [28] Microstructure and Mechanical Properties of Equiatomic CrMnCoNiCu High Entropy Alloy Seung Min Oh, Sun Ig Hong Department of Materials Science and Engineering, Chungnam National University, Daejeon, 34134, Korea